presumably serve to lower the tetragonal–orthorhombic transition temperature. We cannot ascertain where the oxygen is in the structure, but the vacancies within the non-metal framework and the spaces between La atoms in the channels seem possible.

Finally, a dimensional analysis of both LaAlGe and $LaGe_{2-x}$ reveals some interesting facts: (a) the lattice parameters of LaAlGe are significantly larger than those of $LaGe_{2-x}$ even if we extrapolate the calculated volumes of $LaGe_{2-x}$ to "$LaGe_2$", and (b) the c/a ratio of ternary LaGeAl (3.42) is larger than that for the binary (3.38). It must be noted that the axial and chain bonds become identical when $c/a = 2 \tan 60° = 3.464$. Tabulations of lattice parameters for a number of rare-earth-metal disilicides and digermanides with aluminum and transition-metal substitutions[34,36] show similar trends, although the assignment of LaAlGe to the $ThSi_2$-type was erroneous.[33]

(36) Hovestreydt, E.; Engel, N.; Klepp, K.; Chabot, B.; Parthé, E. *J. Less-Common Met.* **1982**, *85*, 247.

Band structure calculations to be reported in a future article[27] consider the nature of the transition between $ThSi_2$- and $GdSi_2$-type structures, the possible electronic effects of Al in the $ThSi_2$ bonding, and the effect of Ge vacancies in $LaGe_{2-x}$.

Acknowledgment. We are much indebted to Professor H. F. Franzen for the use of both the arc-melting furnace and the high-temperature powder diffractometer and for valuable discussions regarding Landau theory.

Registry No. La, 7439-91-0; Al, 7429-90-5; Ge, 7440-56-4; $LaGe_{1.60}$, 136952-84-6; LaAlGe, 12279-56-0; $LaGe_{1.63}$, 136952-85-7; $LaGe_{1.66}$, 136952-86-8; $LaGe_{1.67}$, 136952-87-9; $LaAl_2$, 12004-32-9; $LaAl_{1.75}Ge_{0.25}$, 12279-77-5; $LaAl_{1.5}Ge_{0.5}$, 12279-70-8; $LaAl_{1.25}Ge_{0.75}$, 136952-88-0; $LaAl_{0.75}Ge_{1.25}$, 136952-89-1; $LaAl_{0.5}Ge_{1.5}$, 136952-90-4; $LaAl_{0.25}Ge_{1.75}$, 136952-91-5; $LaAl_{0.2}Ge_{1.8}$, 136952-92-6.

Supplementary Material Available: Tables of data collection and anisotropic atom displacement parameters for $LaGe_{1.60}$ and LaAlGe (2 pages); listings of F_o and F_c data for the two structures (3 pages). Ordering information is given on any current masthead page.

Contribution from the Department of Chemistry,
Iowa State University, Ames, Iowa 50011

Two Novel Titanium Halide Phases: KTi_4Cl_{11} and $CsTi_{4.3}I_{11}$

Jie Zhang, Ru-Yi Qi, and John D. Corbett*

Received April 24, 1991

The title phases were synthesized in high yields from reactions of Ti, $TiCl_3$ or TiI_4, and KCl or CsI, respectively, in sealed tantalum containers at 500–600 °C. Problems associated with the loss of Ti into Ta (or Nb) containers are noted. The structure of each at room temperature was solved and refined by single-crystal X-ray diffraction means. (KTi_4Cl_{11}: *Pnma*, $Z = 4$, $a = 12.534$ (3) Å, $b = 6.897$ (2) Å, $c = 17.134$ (3) Å, $R/R_w = 3.5\%/4.1\%$ for 582 independent reflections with $2\theta \leq 55°$. $CsTi_{4.3}I_{11}$: $P6_3/mmc$, $Z = 2$, $a = 8.2058$ (5) Å, $c = 19.723$ (2) Å, $R/R_w = 2.3\%/2.1\%$ for 181 data, $2\theta \leq 50°$.) The chloride contains infinite chains of tightly bound $Ti_3Cl^i_4Cl^a_5Cl^{a-a}_{4/2}$ clusters [$\bar{d}$(Ti–Ti) = 2.955 Å]. These are interconnected into puckered sheets by isolated titanium(IV) atoms, leaving titanium(II) in the clusters. The isostructural $CsTi_4Cl_{11}$ also exists. The magnetic susceptibility of KTi_4Cl_{11} and the cluster dimensions are quite similar to those reported for the structurally somewhat more complex Ti_7Cl_{16}. The unusual $CsTi_5I_{11}$ structure type can be viewed as a microscopic intergrowth between Ti_3I_8 (defect CdI_2) slabs and layers containing Ti_2I_9 confacial bioctahedra characteristic of $Cs_3Zr_2I_9$ ($Cs_3Cr_2Cl_9$ type). The structure can be easily derived from the latter type. Metal positions in the former (Ti_3I_8) slabs are only 77% occupied, corresponding to a $CsTi_{4.30(7)}I_{11}$ composition but in an apparent line phase. A binary phase near $TiI_{2.5}$ also exists.

Introduction

Although reduced halides of zirconium as well as of rare-earth metals have been found to encompass a plethora of novel cluster-based phases,[1-4] none has been reported for titanium. Our explorations of the latter for a like chemistry, particularly one in which octahedral metal clusters $M_6X_{12}Z$ are stabilized by any of a variety of an essential interstitial elements Z (H, Be–N, Mn–Ni, etc.), have instead demonstrated that reduced titanium halides have a novel structural chemistry of their own. Even though potential interstitial elements Z (in small proportion) have not contributed to a unique chemistry, the remaining TiX_4, Ti, and alkali-metal halide have afforded new phases with, as often happens, unusual structures. We have already reported the $CsTi_2Cl_7$ example, in which $Ti^{III}Cl_6$ clusters are condensed into layers through sharing of five chlorides, leaving a novel Ti=Cl function projecting into the annular space.[5] The present paper reports on two more of these: KTi_4Cl_{11}, in which triangular rather than octahedral metal clusters are formed, and the $CsTi_5I_{11}$ type, which displays intergrown elements of two common structure types. Problems with tantalum as a container for these studies are also noted.

Experimental Section

The synthetic techniques utilizing welded Ta containers and the Guinier powder pattern procedures have already been described.[2-4] The $TiCl_3$ reactant was prepared as before,[5] while TiI_4 was prepared from the elements and purified by vacuum sublimation. The titanium metal was a crystal bar product and was treated as described.[5]

Syntheses. In order to reduce the loss of Ti into the Ta containers (below), a series of reactions designed to make cluster or condensed cluster chloride analogues of other systems were loaded with Ti chips in place of powder and run at 500–550 °C for 40–55 days. The Ti chips in most of the reactions remained intact, and the resultant changes in stoichiometry in one series designed to make $K_xTi_6Cl_{12+y}Z$ products led to, besides Ti, what turned out to be the black KTi_4Cl_{11} as the major and even single product of several reactions.

Reactions of powdered Ti and TiI_4 with a 3d metal M (Cr, Mn, Fe, etc.) and an alkali-metal iodide (AI) designed to synthesize M-centered cluster phases analogous to zirconium examples gave instead several evidently reduced ternary A_xTiI_y phases, the powder patterns of which did not depend on M. Typical reaction conditions were 550–750 °C for 47–26 days, respectively. One pattern for A = Cs looked like that calculated on the basis of the $Cs_3Zr_2I_9$ structure,[7] but the yield was too high considering the input composition, and there were numerous extra weak lines. Once a structural solution established the composition, a

(1) Ziebarth, R. P.; Corbett, J. D. *Acc. Chem. Res.* **1989**, *22*, 256.
(2) Hughbanks, T.; Rosenthal, G.; Corbett, J. D. *J. Am. Chem. Soc.* **1988**, *110*, 1511.
(3) Payne, M. W.; Corbett, J. D. *Inorg. Chem.* **1990**, *29*, 2246.
(4) Zhang, J.; Corbett, J. D. *Inorg. Chem.* **1991**, *30*, 431.
(5) Zhang, J.; Corbett, J. D. *Z. Anorg. Allg. Chem.* **1990**, *580*, 36.
(6) Werner, P. E. TREOR-4: Trial and Error Program for Indexing Unknown Powder Patterns. Department of Structural Chemistry, Arrhenius Laboratory, University of Stockholm, 106 91 Stockholm, Sweden, 1984.
(7) Guthrie, D. H.; Meyer, G.; Corbett, J. D. *Inorg. Chem.* **1981**, *20*, 1192.

0020-1669/91/1330-4794$02.50/0

subsequent 7-day, 600 °C reaction with the overall composition $CsTi_5I_{11}$ gave the new phase in 90% yield as good crystals (black rods) plus TiI_2. Some loss of Ti metal was apparent. Although fractional occupancy of one metal position suggested nonstoichiometry, any range was concluded to be very small, judging from Guinier lattice constants of the phase in equilibrium with either TiI_2 (data crystal) or TiI_3, namely a = 8.2058 (5) vs 8.2001 (5) Å and c = 19.723 (2) vs 19.703 (2) Å, respectively. Excess CsI produces $CsTiI_3$ in the reported hexagonal perovskite structure ($CsNiCl_3$, $P6_3/mmc$) with lattice constants a = 8.178 (2) Å and c = 6.754 (3) Å, which compare with a = 8.205 (5) Å and c = 6.784 (5) Å reported before.[8] Excess titanium metal yields $CsTiI_3$ and TiI_2.

Other Phases. New powder patterns were also seen after A_xTiCl_y reactions at 500–550 °C for A = Li, Na, and Cs, but good crystals were not found, and workable models for the structures could not be located. Analogous iodide phases were repeatedly seen for A = K and Cs but no good crystals. One of the latter was obtained in 95% yield (+CsI) from a reaction stoichiometry corresponding to (the unknown) $Cs_3Ti_2I_9$. The pattern looked a little like a lower symmetry version of that calculated for Cs_2TiI_6[8] in the K_2PtCl_6 type structure that is known for Cs_2ZrI_6.[9] Finally, as noted some years ago,[10] a binary phase near $TiI_{2.5}$ exists although we again have been unable to obtain suitable crystals and a structural solution. The product was obtained in up to 90% yield for a composition $TiI_{2.4}$ after 750 °C for 6 days, the remainder being TiI_3. (Some Ti probably had been lost—see below.) The second phase was TiI_2 (80%) when a reaction composition of $TiI_{2.2}$ was used. TREOR[6] indexing of 11 lines gave a primitive hexagonal cell, a = 3.9327 (1) Å and c = 6.938 (6) Å, which is easily distinguished from TiI_2 dimensions, a = 4.1310 (7) Å and c = 6.825 (2) Å (15 lines). Close-packed iodine dominates the scattering, and Ti positions in the new structure could not be deduced from the powder pattern intensities.

Container Involvement. Product distributions after many reactions made it clear that titanium metal was being lost from the halide systems into the tantalum container, particularly for those run at 700 °C and higher. This had been suggested by earlier work as well but not documented.[11] For example, TiI_4 reactions with powdered Ti at 750 °C for 20 days required overall compositions near TiI before powdered metal could be discerned in the pattern of the product even though TiI_2 is the most reduced phase known. Discoloration or changes in the reflectivity of the inner wall were obvious, particularly where it had been in close proximity to the reactants, and analysis of the container inner wall surface by SEM-EDX after it had been only wiped with acetone-soaked tissue showed appreciable Ti. For example, a reaction of Ti, $TiCl_3$, LiCl, and C with the overall composition $LiTi_6Cl_{15}C$ at 400–500 °C for 40 days plus 550 °C for 15 days left 5–7 atom % Ti in the Ta wall. A niobium container wall with a dark yellow tinge from a comparable reaction for 90 days contained up to 42 atom % Ti. Elimination of any physical contact of the reactants with the Nb container via an intervening Mo sheet did not prove useful at 700 °C (70 days). The Mo exhibited varying but significant Ti contents while Nb therebehind had major Ti contamination that was close to the saturation limit of 85:15 Ti:Nb at the surface and had penetrated about 0.5 mm. Clearly the Ti values are effectively transported by gaseous $TiCl_2$ or $TiCl_3$ and presumably by the analogous iodides as well.

For comparison, the inner wall of a Ta container used for the synthesis of $Cs_2BaZr_6Cl_{18}Ba$ at 800 °C for 15 days showed no detectable Zr therein (<3–5 atom %).

Magnetic Susceptibility. A 59-mg sample of KTi_4Cl_{11} was sealed within a standard fused-silica container under He. The susceptibility was measured at 5 T over the range $6 \le T \le 300$ K on a Quantum Design MPMS SQUID magnetometer.

Structural Studies. KTi_4Cl_{11}. The X-ray powder patterns of this product were indexed by TREOR[6] (36 lines) to an orthorhombic cell 6.26 × 6.89 × 17.13 Å. Although the two smaller values, 6.26 and 6.89 Å, agreed well with those deduced from a zero-level precession photograph on a multiple crystal from the same reaction, this solution was questioned on the basis of crystal proportions. The bladelike morphology of the crystal suggested that the three cell lengths should be significantly different from each other, yet the precession photograph showed that the longest dimension of the crystal corresponded to the 6.89-Å repeat, which ought to be the smallest axis among the three, while the 17.13 Å value was associated with the thickness of the blade. The missed doubling of the 6.26-Å axis oriented along the width of the blade was later shown to have resulted from systematically weak reflections in the powder pattern and systematic absences in the precession photograph.

Table I. Data Collection and Refinement Parameters

formula	KTi_4Cl_{11}	$CsTi_{4.30}I_{11}$
space group, Z	$Pnma$ (No. 62), 4	$P6_3/mmc$ (No. 194), 2
cell params[a]		
a, Å	12.534 (3)	8.2058 (5)
b, Å	6.897 (2)	8.2058 (5)
c, Å	17.134 (3)	19.723 (2)
$2\theta_{max}$, deg	55	50
no. of indep refl	582	181
μ(Mo Kα), cm^{-1}	43.2	178.6
transm coeff range	0.88–1.00	0.57–1.00
R,[b] %	3.5	2.3
R_w,[c] %	4.1	2.1

[a] Guinier powder data, λ = 1.540 56 Å. [b] $R = \sum||F_o| - |F_c||/\sum|F_o|$. [c] $R_w = [\sum w(|F_o| - |F_c|)^2/\sum w(F_o)^2]^{1/2}$; $w = [\sigma(F)]^{-2}$.

After some repetition, the CAD 4 diffractometer finally located 25 reflections that yielded the expected primitive orthorhombic cell. The axial (Polaroid) photograph still indicated a 6.26-Å repeat, but this was ignored in data collection, correctly as it turned out. The Laue group $Pmmm$ was indicated by the raw data, which exhibited the absence conditions $h0k$ ($h + k = 2n$) and $hk0$ ($k = 2n$). This left $P2_1nb$ and $Pmnb$ as possible nonstandard space group candidates. The latter, centrosymmetric example was selected and shown to be correct. An empirical absorption correction based on ψ-scans was applied, and the 2-fold redundant data were averaged with a $3\sigma(I)$ cutoff to give R_{av} = 6.9%. Only about 30% of the measured data were observed. Direct methods (SHELX-86[12]) provided an initial model, which was successfully completed with the aid of standard least-squares full-matrix refinement and Fourier syntheses. However, anisotropic refinement led to nonpositive-definite values for the one metal atom in a general position, while the rest of the atoms behaved rather well. The result was assumed to arise from an absorption problem instead of mistakes in space group determination. A numerical absorption correction (DIFABS[13]) not only solved this but also improved the quality of the entire solution (R_{av} = 5.1%, R = 3.5%, R_w = 4.1%), lowered the residue peaks on the ΔF map, and gave smaller and more uniform ellipsoids for all the other atoms. Refined multiplicities of the one K and three Ti atoms all fell in the range of 99.8 (8)–101.0 (6)%, indicating all metal sites were fully occupied.

$CsTi_5I_{11}$. The structure was solved in a progressive manner. The first crystal from a long 550 °C reaction provided no useful refinement results after data collection in a hexagonal setting until an overexposed Weissenberg photograph revealed weak and diffuse reflections that required doubling of the a and b axes. Data recollection indicated only a 6_3 symmetry axis along c. Direct methods were without success in the indicated $P6_322$ space group, but the orthorhombic subgroup $C222_1$ allowed some progress to be made. Plausible anisotropic refinement results were obtained for all atoms along with residuals of 5.0% and 7.0%; however, the coordinates were close to special positions in trigonal groups and their standard deviations were too large. The structure was redefined in space group $P3$ and then upward in symmetry by removing obvious parameter coupling relationships. This ultimately arrived at $P6_3/mmc$ and a reasonable refinement (4.4%, 7.1%) for effectively the final structure except that numerous weak violations of the c-glide condition had to be ignored, some with $I/\sigma(I) > 10$. Many were next to very strong reflections.

Study of a smaller but better crystal from a 600 °C reaction (above) showed that all of these apparent violations were false and that the model was correct. Reflections in four octants were measured at room temperature to $2\theta \le 50°$, which gave R_{av} = 8.6% for all data in the Laue group $6/mmm$ and 181 independent data with which to refine 25 variables. Absorption was corrected with DIFABS, and the final refinement gave conventional residuals (on F) of 2.3% and 2.1%. The structure type is $CsTi_5I_{11}$, but one titanium atom in a 6g position regularly refined to fractional occupancy, 80 (3)% and 77 (1)% for the two respective data sets. The latter value corresponds to the composition $CsTi_{4.30(7)}I_{11}$.

Some data collection and refinement information for KTi_4Cl_{11} and $CsTi_5I_{11}$ is given in Table I, while the refined coordinates and isotropic equivalent thermal parameters are listed in Tables II and III, respectively. Anisotropic displacement parameters and the structure factor results are available in the supplementary material.

Results and Discussion

Although Ta (or Nb) has proven to be an excellent container for metal–metal halide systems involving Zr, Hf, the rare-earth

(8) Zandbergen, H. W. *J. Solid State Chem.* **1981**, *37*, 308.
(9) Guthrie, D. H.; Corbett, J. D. *Inorg. Chem.* **1982**, *21*, 3290.
(10) (a) Struss, A. W.; Corbett, J. D. *Inorg. Chem.* **1978**, *17*, 965. (b) Cline, J.; Seaverson, L. M.; Corbett, J. D. Unpublished research.
(11) Corbett, J. D. *Inorg. Synth.* **1983**, *22*, 15.
(12) Sheldrick, G. M. SHELXS-86. Institut für Anorganische Chemie, Universität Göttingen, FGR, 1986.
(13) DIFABS: Walker, N.; Stuart, D. *Acta Crystallogr.* **1983**, *A39*, 158.

Table II. Positional and Isotropic Thermal Parameters for KTi_4Cl_{11}[a]

	x	y	z	B_{eq},[b] Å^2
Ti1	0.3201 (2)	1/4	0.6479 (2)	1.12 (5)
Ti2	0.2554 (2)	0.0294 (2)	0.51098 (9)	1.00 (3)
Ti3	0.3256 (2)	1/4	0.8379 (1)	1.00 (5)
K	0.4949 (4)	1/4	0.2424 (5)	4.7 (1)
Cl1	0.1466 (3)	1/4	0.5859 (5)	1.10 (6)
Cl2	0.3371 (3)	1/4	0.4210 (2)	1.24 (7)
Cl3	0.0859 (2)	0.0013 (3)	0.0859 (1)	1.42 (5)
Cl4	0.4748 (3)	1/4	0.7486 (3)	1.56 (6)
Cl5	0.2478 (2)	0.0137 (3)	0.7493 (1)	1.52 (4)
Cl6	0.3261 (3)	1/4	0.0816 (2)	1.28 (7)
Cl7	0.1702 (3)	1/4	0.9244 (2)	1.28 (7)
Cl8	0.0997 (2)	0.0011 (3)	0.4165 (1)	1.26 (5)

[a] Room-temperature data. The refined occupancies of Ti and K atoms were 101.0 (3)%, 100.3 (4)%, 101.0 (6)%, and 99.8 (8)%, respectively. These were fixed at 100% in the final cycles. [b] $B_{eq} = (8\pi^2/3)\sum_i\sum_j U_{ij}a_i^*a_j^*\bar{a}_i\bar{a}_j$.

Table III. Positional and Isotropic Thermal Parameters for $CsTi_{4.3}I_{11}$[a]

	multipl (sym)	x	y	z	B, Å^2
I1	6 (*mm*2)	0.5040 (2)	2*x*	1/4	2.2 (1)
I2	4 (3*m*)	1/3	2/3	0.0819 (1)	2.1 (1)
I3	12 (*m*)	0.1693 (1)	2*x*	0.58447 (6)	2.14 (8)
Cs	2 ($\bar{6}m2$)	0	0	1/4	4.6 (2)
Ti1[b]	6 (2/*m*)	1/2	0	0	2.8 (5)
Ti2	4 (3*m*)	1/3	2/3	0.8324 (4)	2.5 (2)

[a] Room-temperature parameters. [b] Refined occupancy = 0.77 (1).

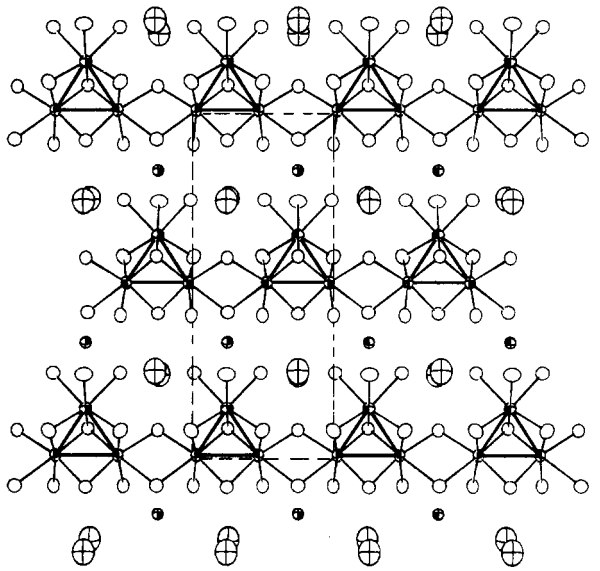

Figure 1. [100] view of one layer in KTi_4Cl_{11} that includes the potassium atoms on both sides. One cell is outlined in projection. Titaniums are shaded, chlorines are open, and potassiums are crossed units (90% probability thermal ellipsoids).

metals, and the alkaline-earth metals,[11] the incorporation of titanium into the container during comparable reactions has proven to be substantial (see Experimental Section). These problems presumably result from the distinctly lower solidus boundaries present in the Ta–Ti and Nb–Ti systems[14] together with a significant mobility. Utilization of Ti as the container would presumably be quite satisfactory for the lowest phases (if transport reactions did not result in excessive wall thinning), but we saw no evidence of any other types of highly reduced phases that would make this worthwhile.

KTi_4Cl_{11}. This unusual compound contains three components: isolated titanium(IV) atoms in octahedral surroundings, chains of Ti_3Cl_{13} cluster units sharing chlorine atoms, viz., $Ti_3Cl_9Cl_{4/2}$,

(14) Massalski, T. B., Ed. *Binary Alloy Phase Diagrams*, 2nd ed.; American Society for Metals: Metals Park, OH, 1990; Vol. 3.

Table IV. Important Distances (Å) and Angles (deg) in KTi_4Cl_{11}

Distances			
Ti1–Ti2 (×2)	2.912 (3)	Ti3–Ti1 (×1)	3.255 (4)
Ti2–Ti2 (×1)	3.042 (2)	Ti3–Cl4 (×1)	2.415 (5)
$\bar{d}$	2.955	Ti3–Cl5 (×2)	2.431 (3)
		Ti3–Cl7 (×1)	2.448 (5)
Ti1–Cl1 (×1)	2.420 (5)	Ti3–Cl8 (×2)	2.386 (3)
Ti2–Cl1 (×2)	2.413 (3)	$\bar{d}$(Ti3–Cl)	2.416
Ti2–Cl2 (×2)	2.396 (3)		
Ti1–Cl3 (×2)	2.349 (3)	K–Cl2 (×1)	3.643 (8)
Ti2–Cl3 (×2)	2.377 (3)	K–Cl3 (×2)	3.591 (8)
$\bar{d}$(Ti–Cl^i)	2.388	K–Cl4 (×2)	3.473 (8)
		K–Cl5 (×2)	3.706 (5)
Ti1–Cl4 (×1)	2.595 (5)	(×2)	3.546 (5)
Ti1–Cl5 (×2)	2.548 (3)	K–Cl6 (×1)	3.473 (8)
Ti2–Cl6 (×2)	2.495 (3)	K–Cl8 (×2)	3.477 (7)
Ti2–Cl7 (×2)	2.605 (3)	$\bar{d}$	3.559
Ti2–Cl8 (×2)	2.543 (3)		
$\bar{d}$(Ti–Cl^a)	2.553		
Cl3–Cl4	3.369 (5)[a]	Cl6–Cl7	3.328 (5)
Cl4–Cl5 (×2)	3.279 (4)	Cl7–Cl8	3.367 (4)
Cl5–Cl5	3.259 (3)		

Angles			
Ti2–Ti1–Ti2 (×1)	62.99 (7)	Ti2–Cl7–Ti2	95.4 (1)
Ti1–Ti2–Ti2 (×2)	58.50 (5)	Cl3–Ti1–Cl5	163.4 (1)
Ti1–Cl1–Ti2 (×2)	74.1 (1)	Cl3–Ti2–Cl8	168.3 (1)
Ti2–Cl1–Ti2 (×1)	78.2 (1)	Cl2–Ti2–Cl6	167.9 (1)
Ti2–Cl2–Ti2 (×1)	78.8 (1)	Cl1–Ti2–Cl7	166.4 (1)
Ti1–Cl3–Ti2 (×2)	76.1 (1)	Cl1–Ti1–Cl4	164.4 (2)
Ti2–Cl6–Ti2	101.2 (1)		

[a] d(Cl–Cl) < 3.40 Å.

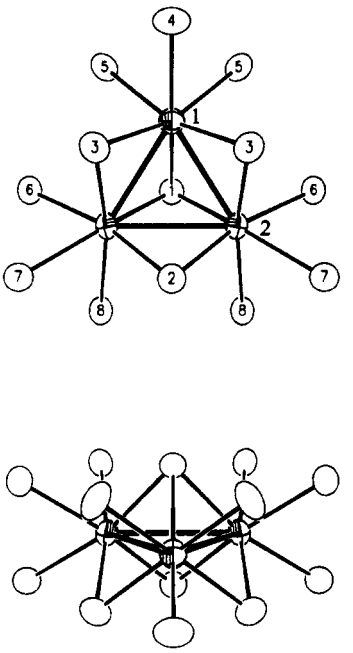

Figure 2. [100] (top) and [001] (bottom) views of the cluster unit in KTi_4Cl_{11} with the atom-numbering scheme. The orientation at the top is the same as in Figure 1.

and potassium ions. The overall structure is shown in Figure 1, while the dimensions are listed in Table IV. The familiar construction of the triangular Ti_3Cl_{13} clusters is shown in two views in Figure 2. These are readily described either as titanium atoms enclosed in three adjoining octahedral sites between close-packed chlorine layers or as three $TiCl_6$ octahedra each of which shares a pair of Cl^i edges, one vertex being common to all three, viz., $Ti_3Cl^i_{3/3}Cl^i_{6/2}Cl^a_9$. These Ti_3Cl_{13} cluster units are then condensed into chains through sharing of four $Cl^{a\text{-}a}$ atoms (Cl6 and Cl7) per cluster to produce $Ti_3Cl^i_4Cl^a_5Cl^{a\text{-}a}_{4/2}$, as shown in Figure 1. Finally, the five remaining terminal Cl^a atoms Cl4, Cl5(×2), and Cl8(×2) plus the intercluster bridging Cl7 are also bonded to the isolated Ti3 atoms that serve to join the chains into puckered sheets. These last bonds to Ti3 are not shown in Figure 1. All chlorines are

bonded to two titanium atoms except for the centered Cl1 and bridging Cl7 which have three metal neighbors. The chains in Figure 1 occur with alternative orientations of the capping Cl1 atoms. A puckering within the layers results from alternate rotations of adjoining chains, roughly by ±20° about the Ti2–Ti2 edges, so as to generate suitable trigonal-antiprismatic cavities for the isolated Ti3 atoms.

Finally, potassium occurs in 12-coordinate sites between the layers and appears to be the least demanding of the structural components. The three-bonded Cl1 and Cl7 atoms mentioned above are, logically, not neighbors to K. The average d(K–Cl) of 3.56 Å is noticeably greater than the sum of crystal radii, 3.45 Å,[15] even though titanium is the backside neighbor to chlorine. The overly large cavity presumably is responsible for the larger thermal ellipsoids for potassium (4.7 Å^2 vs 1.25 Å^2 average for others). This suggested that ATi_4Cl_{11} phases with larger cations should also form this structure, and the synthesis of $CsTi_4Cl_{11}$ was subsequently accomplished, the largest change in dimensions naturally being in the interlayer separations along $\vec{a}$ (a = 12.82 Å, b = 6.96 Å, c = 17.15 Å).

As is common in many other solid-state compounds, KTi_4Cl_{11} can also be described in terms of close-packed layers that lie normal to $\vec{c}$ and to the sheets shown in Figure 1. The orientation sequence is ABACBC or $(chc)_2$, reflecting the local structure of the cluster chains; one-third of the layers have a KCl_3 composition and the remainder contain only chlorine.

The local structure of the trimetal cluster in KTi_4Cl_{11} appears somewhat unusual. The isolated metal atom (Figure 1) is to a first approximation reasonably assigned as titanium(IV). This is consistent with the fact that all but one of the five shortest Cl···Cl distances are within this polyhedron. On the other hand, both the distances and angles within the Ti_3 cluster suggest significant bonding interactions between the formally titanium(II) atoms. The metal atoms are clearly displaced from the octahedral centers *toward* each other (Figure 2, bottom), a longstanding criterion[16] for a bonding interaction and in opposition to the repulsion expected for like-charged cations. The average d(Ti–Ti), 2.955 Å, corresponds to a Pauling bond order of 0.30 per edge, and the six d electrons assignable to the cluster could lead to nominal single bonds along the edges of the triangle. However, a sizable matrix effect arising from the dissimilar sizes of Ti and Cl and the required distortions of the octahedra would be expected to hinder the realization of anything near the ultimate Ti–Ti bonding. The distortion may be responsible for the short intracluster Ti–Cl^i bonds which average 2.39 Å, in contrast to those from cluster Ti to Cl^a atoms that either bridge to the isolated Ti3 atom or to other clusters in the chain which average 2.55 Å. The former value is in fact comparable to the average about the isolated Ti3, 2.42 Å. The 3.255 (4) Å distance between the lone Ti3 and Ti1 in the cluster through a shared octahedral face (bond order = 0.09) does not seem to present any trouble in the model; a repulsion is more probable than bonding since the Ti1 atom in the cluster has moved away.

The Ti_3Cl_{11} cluster repeat units in KTi_4Cl_{11} are remarkably similar to those in Ti_7Cl_{16} and Ti_7Br_{16}[17,18] reported a few years ago. These contain the same $[Ti_3X^i_2X^a_5X^{a-a}_{4/2}]$ chains, but pairs of these are linked by isolated Ti(IV) atoms into $Ti[Ti_3X_{11}]_2$ double chains, and these are further bonded in a complex three-dimensional way through sharing of the equivalent of the Cl5^a and Cl4^a atoms shown here. The two chloride clusters are still very similar, particularly with respect to the distortion of the shared $TiCl_6$ octahedra, and the metal triangles have the same average d(Ti–Ti). In addition, the short (or crowded) Ti–Cl^i distances are closely comparable, 2.382 Å vs 2.388 Å here (Table IV), while the larger Ti–Cl^a values differ a little, averaging 2.59 Å vs 2.53 Å here, with a smaller range. The isolated titanium(IV) atoms do exhibit somewhat different Ti–Cl bond distances, however, 2.549 Å vs 2.416 Å here, but this may have something to do with the more complex bridging in Ti_7Cl_{16}. Notwithstanding, it seems clear that triangular Ti_3X_{13}-type clusters do exhibit a significant stability and can function as "building blocks" in more than one structure type.

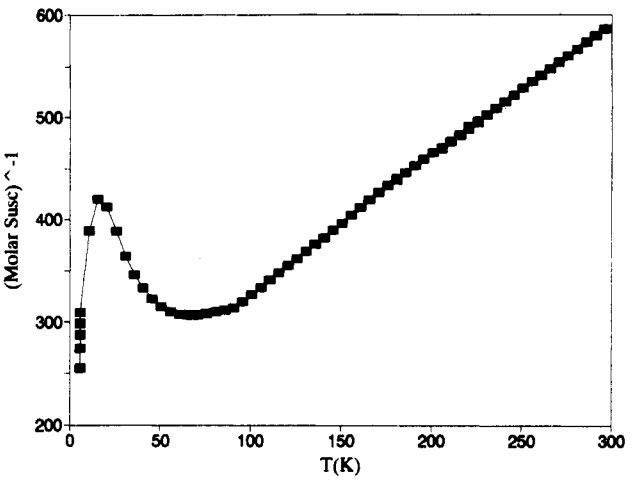

Figure 3. Molar magnetic susceptibility of KTi_4Cl_{11} at 5 T. The first five points at the lowest temperature are data taken at 1–5 T in unit steps.

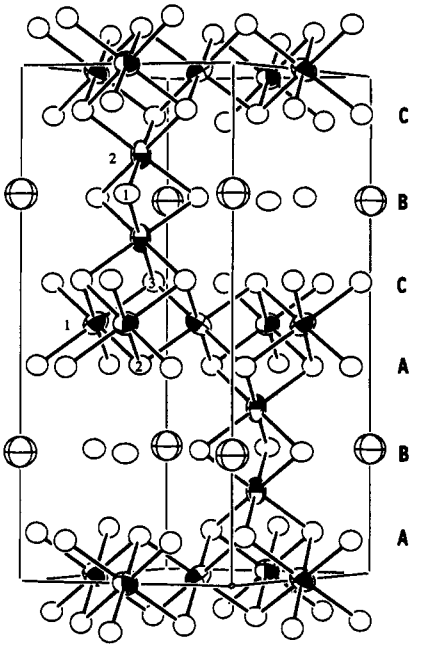

Figure 4. An approximately [110] view of the cell contents of $CsTi_5I_{11}$ with $\vec{c}$ vertical and the layering sequence and the atom numbers identified. Titaniums are shaded, iodines are open, and cesiums are crossed (90%) ellipsoids.

A close relationship between the clusters in the two structures is also indicated by their comparable magnetic data. The inverse molar susceptibility of KTi_4Cl_{11} is shown in Figure 3 as a function of temperature. The linear portion corresponds to a moment of 2.46 μ_B per formula unit with a Weiss constant of −150 K, although these values may not be particularly meaningful because of the evident strong coupling. A detailed magnetic study of Ti_7X_{16} (X = Cl, Br) has been provided by Lueken and Maqua.[19] Ti_7Cl_{16} exhibits magnetic properties remarkably similar to those of KTi_4Cl_{11} but with evidently greater coupling, as reflected in a smaller slope, a larger Weiss constant (∼−210 K), and a larger maximum at ∼21 K. The earlier investigators interpreted their data in terms of a substantially reduced g value (1.11), a Van Vleck temperature-independent term, a temperature-dependent antiferromagnetic exchange parameter J (60–30 cm^{-1}), and an

(15) Shannon, R. P. *Acta Crystallogr.* **1976**, *A32*, 751.
(16) Schäfer, H.; Schnering, H.-G. *Angew. Chem.* **1964**, *76*, 833.
(17) Schäfer, H.; Laumann, R. *Z. Anorg. Allg. Chem.* **1981**, *474*, 135.
(18) Krebs, B.; Henkel, G. *Z. Anorg. Allg. Chem.* **1981**, *474*, 149.
(19) Lueken, H.; Maqua, L. *Z. Anorg. Allg. Chem.* **1982**, *490*, 64.

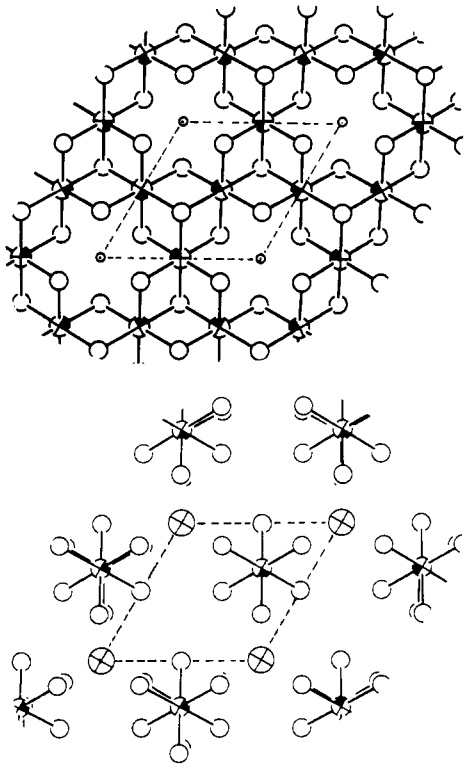

Figure 5. [001] views of the Ti_3I_8 slab AC (top) and the $Cs_3Ti_2I_9$-like slab about B (bottom) to show their stacking in $CsTi_5I_{11}$. The atom identifications are the same as in Figure 4 (95% ellipsoids).

intercluster coupling parameter. They concluded that the isolated titanium atoms were fully oxidized, and there was strong antiferromagnetic coupling both within and between the titanium(II) clusters. However, the magnetic behavior of either phase does not provide much direct information about the *bonding* interactions that give rise to such clear distortions within the individual clusters, an effect that the earlier analysis did not address. A reconsideration of the magnetic properties is warranted.

$CsTi_5I_{11}$. The view of the cell in this structure type shown in Figure 4 immediately suggests a remarkable arrangement, an intergrowth of TiI_2 (CdI_2)-like slabs with sections of a $Cs_3Ti_2I_9$ ($Cs_3Cr_2Cl_9$-type) phase in which there are isolated confacial octahedral dimers like that shown. Although $Cs_3Ti_2I_9$ appears to be unknown, $Cs_3Zr_2I_9$ is a closely related model.[7]

The structure can be viewed in terms of close-packed layers with a sequence normal to *c* of ABACBC (or $(chc)_2$) in which the AC pairs are CdI_2-like and the CsI_3 layer B is centered in the Ti_2I_9 dimer. This can be seen better in projection in Figure 5, which shows that the CdI_2-like layers actually have the composition $(Ti1)_3(I2)_2(I3)_6 = Ti_3I_8$, and the CsI_3 layers are positioned so that the cation vacancies in the former occur above and below the cesium atoms. (The Ti_3I_8 layers are like those in Nb_3X_8[20] except that the titanium atoms remain in the ideal centers of the iodine antiprisms.) Thus, Figure 4 is easier to visualize when it is noted that the Ti1 atoms in the Ti_3I_8 layers have the same projection as I1 in the CsI_3 layers, and the Ti2 atoms in the bioctahedra, the same projection as I2 on the far side of the bilayers. A second pair of bioctahedra centered at $^1/_3, ^2/_3, ^1/_4$ and $^2/_3, ^1/_3, ^3/_4$ is not possible as these are centers of confacial *tetrahedra* with I2 apices. Although the Ti_3I_8 layers contain $Ti_3I_4I_9$ groups as found in KTi_4Cl_{11} and elsewhere, these now share metal vertices and iodine within the nets without distinction.

Table V. Important Distances (Å) and Angles (deg) in $CsTi_{4.3}I_{11}$

		Distances	
Ti1–Ti1 (×4)	4.1029 (3)	Cs–I1 (×6)	4.1033 (3)
Ti2–Ti2 (×1)	3.25 (2)	Cs–I3 (×6)	4.055 (1)
Ti2–Ti1 (×3)	4.067 (6)	I1–I1[a] (×2)	4.004 (4)
Ti1–I2 (×2)	2.867 (1)	I1–I3 (×4)	4.006 (1)
Ti1–I3 (×4)	2.8811 (9)	I2–I3 (×3)	4.026 (2)
Ti2–I1 (×3)	2.825 (5)	I3–I3 (×2)	4.039 (3)
Ti2–I3 (×3)	2.851 (5)		
		Angles	
I2–Ti1–I2	180	I1–Ti2–I1	90.2 (2)
I2–Ti1–I3	88.91 (3)	I1–Ti2–I3	89.78 (2)
I3–Ti1–I3	180	I3–Ti2–I3	90.2 (2)
I3–Ti1–I3	90.99 (6)	Ti2–I1–Ti2	70.2 (3)

[a] d(I–I) < 4.05 Å.

The actual composition of this compound, which appears to be substantially a line phase, is $CsTi_{4.30(7)}I_{11}$, the Ti1 positions in the bilayers regularly refining to only ~77% occupancy. This increases the average oxidation state from +2 to +2.33 or gives either type of metal an oxidation state of +2.6 to +2.7 if the other type is titanium(II).

Iodine atoms in the Ti_3I_8 layers are all three-bonded because of the Ti_2I_9 units condensed thereon. The average Ti1–I distance in the layers is 2.876 Å, the same as the crystal radius sum for six-coordinate Ti(III), 2.87 Å.[15] The Ti2–I1 distances in the center of the dimers, 2.825 (5) Å, are slightly less than at the ends, Ti2–I3 = 2.851 (5) Å. The meaning of this is somewhat obscured by the fact that the former I1 atoms all have only two titanium neighbors, not three (plus two Cs neighbors), and are thereby naturally closer to Ti2. The Ti2–Ti2 distance in this dimer, 3.25 Å (bond order = 0.09), scarcely seems meaningful; all other Ti–Ti separations are over 4 Å.

The Ti–I–Ti angle (β) at I1 in the bridge in Ti_2I_9 units, 70.2°, is virtually ideal for two octahedra sharing a face, which requires 70.53°. As summarized earlier,[7] all other known M_2X_9 units are distorted because of the significant differences in halogen coordination in the bridge relative to that at the ends of the discrete dimers. M_2X_9 units with M–M bonding exhibit β angles in the range 60–65°, while those without significant M–M interactions or weak repulsions (because of smaller X, larger M, or no valence electrons) give β's in the range 76–81°.

Finally, the conceptual relationship of the $CsTi_5I_{11}$ structure type to the hypothetical $Cs_3Ti_2I_9$ ($Cs_3Zr_2I_9$ or $Cs_3Cr_2Cl_9$ type) is actually closer than might be apparent. Both exhibit the same space group and cell proportions. For the conversion of $Cs_3Ti_2I_9$ to the stoichiometric $CsTi_5I_{11}$, both iodines, one cesium (2b), and the titanium position are retained, while the second cesium (4f) is converted to the nominally isoelectronic I2. Charge balance requires the insertion of the additional, but light, dipositive Ti1 (also 4f) within what are now the I2,I3 bilayers. In this light, it is not at all surprising that the powder pattern calculated for the unknown $Cs_3Ti_2I_9$ on the basis of the $Cs_3Zr_2I_9$ positional parameters looks so much like that observed for $CsTi_5I_{11}$.

Acknowledgment. We are indebted to J. Ostensen for the magnetic data on KTi_4Cl_{11}. This research was supported by the National Science Foundation, Solid State Chemistry, via Grant DMR-8902954.

Supplementary Material Available: Tables of data collection parameters and atomic anisotropic displacement parameters for KTi_4Cl_{11} and $CsTi_5I_{11}$ (2 pages); listings of structure factor data for the same compounds (6 pages). Ordering information is given on any current masthead page.

(20) Simon, A.; von Schnering, H.-G. *J. Less-Common Met.* **1966**, *11*, 31.